

doi:10.15199/48.2022.08.08

## Three phase MLI implementation of V/F control for three phase induction motor based on FPGA and Gary wolf algorithm

**Abstract:** Due to their efficient characteristics multilevel inverters (MLI) find numerous applications in industry. In this work design and implementation of three phase 15 level inverter is used to control the speed of three phase induction motor with V/F strategy. The power circuit consist of 10 MOSFET switches per phase. Spartan 3E FPGA kit is used as a control circuit. The triggering angles for the thirty MOSFET power transistor are determined with optimum values based on gray wolf optimization algorithm (GWO). Results in the form of output voltage, current, speed, and torque are shown for different reference speeds. The torque is shown to be constant as expected for all speeds. The total harmonic distortion (THD) is reduced to a significant value compared with a traditional sinusoidal PWM technique.

**Streszczenie.** Ze względu na swoją wydajność, falowniki wielopoziomowe (MLI) znajdują liczne zastosowania w przemyśle. W pracy wykorzystano projekt i wykonanie trójfazowego falownika 15-stopniowego do sterowania prędkością trójfazowego silnika indukcyjnego ze strategią V/F. Obwód zasilający składa się z 10 przełączników MOSFET na fazę. Jako obwód sterujący zastosowano zestaw Spartan 3E FPGA. Kąty wyzwalania dla trzydziestu tranzystorów mocy MOSFET są określone z optymalnymi wartościami w oparciu o algorytm optymalizacji szarego wilka (GWO). Wyniki w postaci napięcia wyjściowego, prądu, prędkości i momentu obrotowego są wyświetlane dla różnych prędkości odniesienia. Pokazano, że moment obrotowy jest stały, zgodnie z oczekiwaniami dla wszystkich prędkości. Całkowite zniekształcenia harmoniczne (THD) są zredukowane do znaczącej wartości w porównaniu z tradycyjną techniką sinusoidalnego PWM. (Trójfazowa implementacja MLI sterowania V/F dla trójfazowego silnika indukcyjnego w oparciu o FPGA i algorytm Gary wolf)

**Keywords:** V/F, induction motor, FPGA, GWO

**Słowa kluczowe:** przetwornik V/F, FPGA, algorytm szarego wilka

### 1. Introduction

The inverter normally outputs two voltage levels, positive and negative levels and is called two-level inverter. The inverter output voltage can be synthesized by more than two voltage levels for high power applications and is called multilevel inverters (MLI) and offers better sinusoidal voltage waveform and lower THD compared with two-level inverters. In recent years, MLI have gained popularity as power converters of choice in a variety of applications. Because of their capacity to eliminate undesired harmonics and hence enhance performance and efficiency, they have substantial advantages over traditional ones. The reduction of cost and size of the inverter and improves the reliability as minimum number of power electronic components is involved. Several topologies for realizing these inverters have lately been introduced and researched [1-5]. In general, induction motors are one of the very important things in our daily life, as the induction motor disturbs all our daily and industrial lives, due to the many attractive features that the motor possesses, as it has proven that it has a very high reliability in all the matters used, and its advantages are also low price and ease in maintenance. MLI is used in many fields, including driving, to control induction motors, and it has proven its high ability to control frequency and voltage, and there are many published researches in this field. Various methods to control the frequency and voltage of induction motors is tackled [6-8]. One of the advantages of MLI is its ability to improve the value of the THD as well, through which the outgoing wave approaches the shape of the sine wave, and in this case the value of the THD will decrease [9-12]. In this manner the circuit has high implementation flexibility, high efficiency, and high usage of the output voltage [13-14]. Reducing the number of switches used and DC sources compared to the traditional H bridge, modern technologies reduce the number of switches with the largest possible number of levels and there are many topologies used that have proven its efficiency [15-17]. The reduction of THD and elimination of undesired harmonics require selecting accurate triggering instants to control the operation of the MOSFET switches in MLI using efficient optimization algorithms. In this work the

values of the triggering angle for the power switches of the inverter are found by using GWO, which uses the gray wolf hunting theory to solve mathematical equations [18]. This optimization algorithm assists to reduce and eliminate the desired harmonics and as a result the THD value will be improved. MLI are one of the most extensively used power conversion devices in industrial applications. Motor drives of all voltage and power ratings make up most of these applications. In grid-connected systems, such as uninterruptible power supply (UPS), electric vehicles, and FACTS devices, MLIs are also employed [19]. All these applications are made possible by the MLI's ability to provide a higher output voltage with a more sinusoidal shaped waveform, increased efficiency due to the lower switching frequency operation of switches, smaller blocking voltage requirement with reduced dv/dt, and managed to improve electromagnetic compatibility. MLI also has the advantage of reducing the size and cost of the filter due to the lower number of harmonics at the output [20-23].

### 2. Three phase induction motor V/F speed control

There are several methods for controlling the speed of a three-phase induction motor, including stator voltage control, frequency control, and rotor resistance control, but V/F speed control is the most widely used method in adjustable speed drive systems. The V/F ratio must be kept constant for the flux to remain constant. The motor torque is proportional to the magnetic field created by the stator. To analyze the factors that influence the motor's magnetic flux, the flux is formed when ac voltage is applied to the stator of an induction motor, and the flux is in phase with the applied voltage.

$$\Phi = \Phi_m \sin \omega t$$

The generated EMF in the stator according to Faraday's electromagnetic induction is expressed as:

$$\begin{aligned} e &= -N \frac{d\Phi}{dt} \\ e &= 2\pi f N \Phi_m \cos \omega t \\ e &= E_m \cos \omega t \end{aligned}$$

where

$$E_m = 2\pi f N \Phi_m$$

$$E_{rms} = \frac{E_m}{\sqrt{2}}$$

$$E_{rms} = 4.44 \Phi_m f N$$

$$\Phi_m = \frac{E_{rms}}{4.44 f N}$$

$$\Phi_m = V/f$$

(2)

thus, the flux generated in the stator depends on the ratio of the Volt/Hz. As a result, the torque may be kept constant across the speed range by adjusting the voltage and frequency by the same ratio. Torque of a three-phase induction motor is proportional to flux per stator pole, rotor current and power factor of the rotor

$$T = k \Phi I_2 \cos \theta_2$$

(3)

Where  $\Phi$  = flux per stator pole;  $I_2$  = rotor current at standstill;  $\theta_2$  = angle between rotor emf and rotor current

The most common speed control of induction motor is the constant ratio of V/f [24-26]. The voltage and frequency values must be stored for continuous V/F control. It is simple to calculate the voltage value that corresponds to any frequency. The maximum torque of the motor becomes constant for various speed values when the V/F ratio is kept constant [27-28]. Figure (1) shows the linear region of allowed operation for minimum and maximum(rated) frequencies along with corresponding input voltages. The rated voltage meets the maximum frequency. The torque is kept constant in this region. If the frequency exceeds the maximum one the torque is dramatically falling beyond maximum torque. The speed of the motor is proportional to the frequency

$$N = \frac{120P}{f}$$

(4)

where P is number of pair of poles of the motor. If the motor is rated at 400V, 50Hz, 1500rpm, then to half the rated speed, the voltage and frequency must be 200V, 25Hz respectively to keep the flux constant so that we can keep the torque at maximum value.

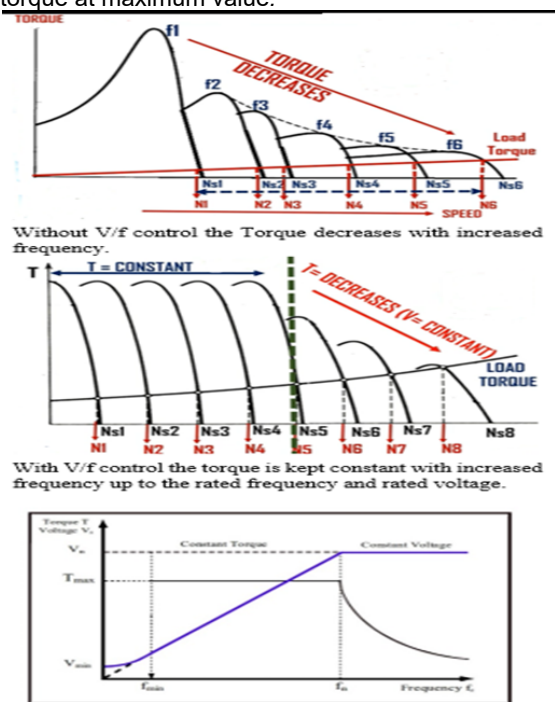


Fig.1. Voltage/frequency characteristics

### 3. Control method for the proposed three phase MLI

Conversion of DC power to three phase AC power with the desired output voltage and frequency is the job of three phase inverters. Three phase MLI's output's high voltages that are very close to the shape of AC voltages and minimize the THD contents of the power. The three-phase MLI block diagram is shown in figure (2).

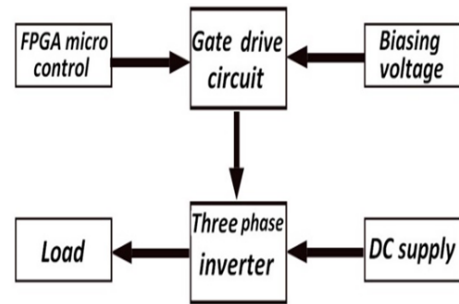


Fig.2. Block diagram of three phase VSI

The GWO is used in this work to optimize the triggering angles for minimum THD values. The three phase MLI consists of three groups of switches, each group represents a phase, and each phase contains 10 switches and four DC sources. As shown in figure (3). The first source is  $V_{dc1}$  and three other sources are  $V_{dc2} = 2V_{dc1}$ . In this way of connection, the three-phase inverter outputs 15 voltage levels per phase. The proposed three-phase power circuit consists of thirty MOSFET's switches and 12 DC sources. A 3E spartan FPGA hardware kit is used as the drive circuit to trigger the MOSFETs in the three-phase MLI.

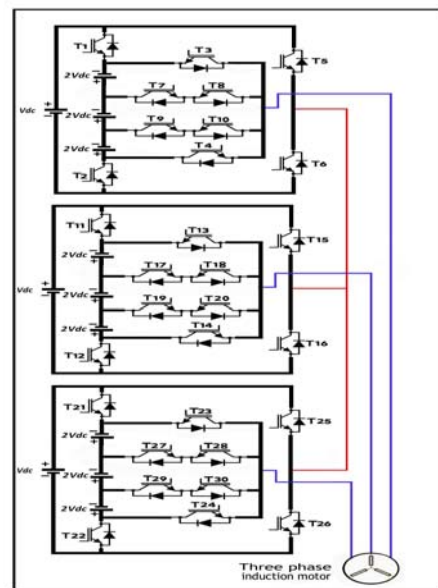


Fig.3. The proposed three-phase MLI circuit

#### 3.1 Gray wolf (GWO) optimization algorithm

The GWO is a new meta-heuristic inspired by grey wolves. The GWO algorithm mimics the leadership hierarchy and hunting mechanism of grey wolves in nature. Four types of grey wolves such as alpha, beta, delta, and omega are employed for simulating the leadership hierarchy. In addition, the three main steps of hunting, searching for prey, encircling prey, and attacking prey, are implemented. The algorithm is then benchmarked on 29 well-known test functions, and the results are verified by a comparative study with Particle Swarm Optimization (PSO), Gravitational Search

Algorithm (GSA), Differential Evolution (DE), Evolutionary Programming (EP), and Evolution Strategy (ES). The results show that the GWO algorithm can provide very competitive results compared to these well-known meta-heuristics [29-31].

### 3.2 Fiarrayprogrammable gate FPGA control circuit

The FPGA microcontroller of the Spartan 3E is used to get the triggering angles for the MOSFET switches. The kit clock frequency is 50MHz allows an efficient sampling rate. The output ports can be easily extended to get the required thirty triggering angles. The VHDL language is adopted to write the instructions that accurately outputs the thirty triggering angles for the power MOSFET's. At first, these triggering angles are obtained from GWO algorithm by solving the following transcendental equations to eliminate undesired harmonics, then programmed by ISE software, then projected onto the 3E Spartan FPGA microcontroller. To output 15 levels we need to solve seven transcendental equations for the optimum seven angles i.e. ( $\alpha_1, \alpha_2, \alpha_3, \alpha_4, \alpha_5, \alpha_6, \text{ and } \alpha_7$ ) for minimum THD. Considering  $V_M$  as the fundamental component :

$$(5) \frac{4V_{dc}}{\pi} [\cos\alpha_1 + \cos\alpha_2 + \cos\alpha_3 + \cos\alpha_4 + \cos\alpha_5 + \cos\alpha_6 + \cos\alpha_7] = V_M$$

$$\frac{4V_{dc}}{5\pi} [\cos5\alpha_1 + \cos5\alpha_2 + \cos5\alpha_3 + \cos5\alpha_4 + \cos5\alpha_5 + \cos5\alpha_6 + \cos5\alpha_7] = 0$$

$$\frac{4V_{dc}}{7\pi} [\cos7\alpha_1 + \cos7\alpha_2 + \cos7\alpha_3 + \cos7\alpha_4 + \cos7\alpha_5 + \cos7\alpha_6 + \cos7\alpha_7] = 0$$

$$\frac{4V_{dc}}{11\pi} [\cos11\alpha_1 + \cos11\alpha_2 + \cos11\alpha_3 + \cos11\alpha_4 + \cos11\alpha_5 + \cos11\alpha_6 + \cos11\alpha_7] = 0$$

$$\frac{4V_{dc}}{13\pi} [\cos13\alpha_1 + \cos13\alpha_2 + \cos13\alpha_3 + \cos13\alpha_4 + \cos13\alpha_5 + \cos13\alpha_6 + \cos13\alpha_7] = 0$$

$$\frac{4V_{dc}}{17\pi} [\cos17\alpha_1 + \cos17\alpha_2 + \cos17\alpha_3 + \cos17\alpha_4 + \cos17\alpha_5 + \cos17\alpha_6 + \cos17\alpha_7] = 0$$

$$\frac{4V_{dc}}{19\pi} [\cos19\alpha_1 + \cos19\alpha_2 + \cos19\alpha_3 + \cos19\alpha_4 + \cos19\alpha_5 + \cos19\alpha_6 + \cos19\alpha_7] = 0 \dots\dots\dots$$

Using GWO to solve equation (5) will eliminate 5<sup>th</sup>, 7<sup>th</sup>, 11<sup>th</sup>, 13<sup>th</sup>, 17<sup>th</sup>, and 19<sup>th</sup>, while the triplane harmonics are eliminated explicitly in the three phase inverter outputs i.e.(3<sup>rd</sup>, 9<sup>th</sup>, 15<sup>th</sup>, 21<sup>st</sup>) and so forth. As a result, the first harmonic to show is 23<sup>rd</sup>.

### 3.3 three phase layout circuit

Four DC voltage sources are used in each single phase. They are  $V_{DC}$  and three equal values of  $2V_{DC}$  to get a 15-level single phase inverter. This arrangement is repeated three times to get three phase MLI. The required  $120^\circ$  between the three phases are implemented by VHDL programming in FPGA microcontroller. The different levels output voltage from the suggested technique is determined by proper operation of the MOSFET power switches T1 through T30 which are connected directly to dc sources. The line-to-line voltages, for instance  $v_{ab} = v_{an} - v_{bn}$  consists of 25 levels, and this makes the output wave form closer to the shape of the sine wave.

### 3.4 Modes of operation

The proposed system generates 15 level output phase voltages as:

$$V_{DC}, 2V_{DC}, 3V_{DC}, 4V_{DC}, 5V_{DC}, 6V_{DC}, 7V_{DC}, 0, -V_{DC}, -2V_{DC}, -3V_{DC}, -4V_{DC}, -5V_{DC}, -6V_{DC}, -7V_{DC}$$

Table (1) summarizes how to operate the MOSFET switches to get all the mentioned modes of operation.

Table 1. Switches states for different output levels

Voltage	T1	T2	T3	T4	T5	T6	T7	T9
0	1	0	1	0	1	0	0	0
Vdc	1	0	1	0	0	1	0	0
2Vdc	1	0	0	0	1	0	1	0
3Vdc	1	0	0	0	0	1	1	0
4Vdc	1	0	0	0	1	0	0	1
5Vdc	1	0	0	0	0	1	0	1
6Vdc	1	0	0	1	1	0	0	0
7Vdc	1	0	0	1	0	1	0	0
0	0	1	0	1	0	1	0	0
-Vdc	0	1	0	1	1	0	0	0
-2Vdc	0	1	0	0	0	1	0	1
-3Vdc	0	1	0	0	1	0	0	1
-4Vdc	0	1	0	0	0	1	1	0
-5Vdc	0	1	0	0	1	0	1	0
-6Vdc	0	1	1	0	0	1	0	0
-7Vdc	0	1	1	0	1	0	0	0

Figure (4) shows all the fifteen output voltage levels with its corresponding MOSFET's switching states.

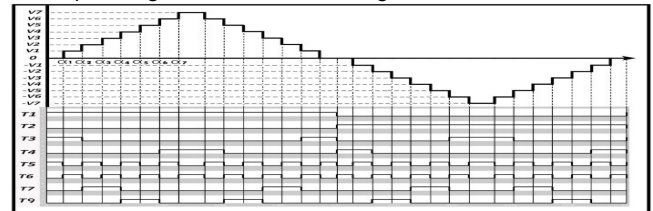


Fig.4. the proposed fifteen output voltage levels

Figure (5) shows the implantation of the triggering angles on the 3E spartan FPGA kit for 15 level three-phase MLI



Fig.5. 3E Spartan MLI control signals wit corresponding switching states

Figure 6 clarifies the modes of operation for the possible seven positive levels along with the zero level.

## 6. Experimental results

The hardware set for the three-phase MLI implementation of V/F control of the three-phase induction motor based on FPGA and GWO algorithm is shown in figure 7.

The three-phase MLI must fulfill the voltage to frequency ratio to be constant, for instance at the rated speed of 1500rpm, the rated voltage  $V_{ph} = 220V$  and the operating frequency  $f = 50Hz$ . These values make the ratio  $(V/F) = 220/50$  which outputs a certain value of flux  $\Phi$  and in turn a certain value of maximum torque. To half the rated speed, i.e. 750rpm, the ratio must be  $(V/F) = 110/25$ , this will ensure the same value of flux  $\Phi$  and the same value of maximum torque. The appropriate triggering instants for each case are determined by the GWO optimization method and then the hardware of the 3E Spartan FPGA kits output the

required triggering instants and deliver them to the appropriate MOSFET's transistor. Table (2) shows the triggering instants for three V/F control as determined by GWO algorithm.

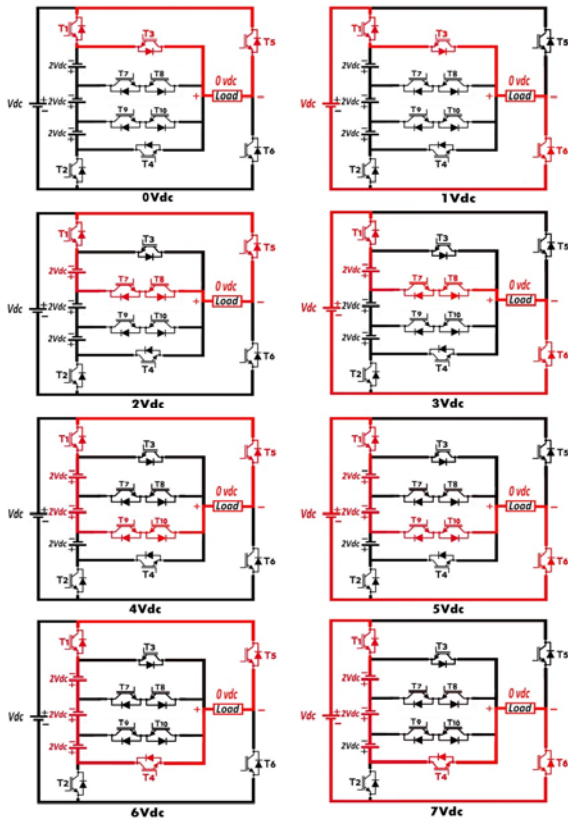


Fig.6. Positive and zero levels operation modes

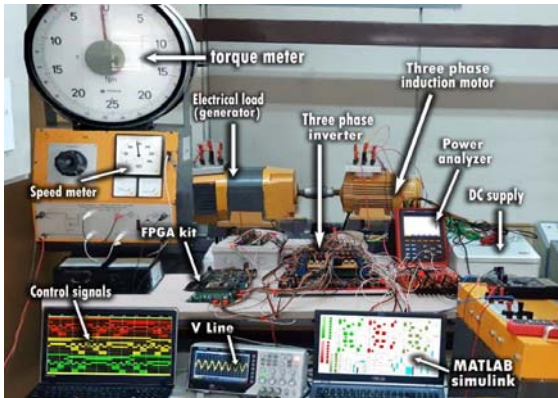


Fig.7. Practical set for the proposed work

Table 2. The triggering instants for three V/F control

		$\alpha_2$	$\alpha_3$	$\alpha_4$	$\alpha_5$	$\alpha_6$	$\alpha_7$
	4.0	12.5	21.1	29.8	39.8	51.6	67.2
70/35	20.1	30.0	40.6	52.5	60.8	76.4	89.7
50/25	30.0	38.6	48.5	70.5	85.8	88.4	89.7

The motor specifications are 5.4Hp 4KW,400V,50Hz, 1430 RPM. Stator resistance and inductance  $R_s = 1.405\Omega$ ,  $L_s=0.0058H$ , rotor resistance and inductance  $R_r=1.395\Omega$ ,  $L_r=0.0058H$ , mutual inductance  $=0.1722H$ , inertia  $J=0.0131 \text{ kg.m}^2$ , friction factor  $F=0.002985 \text{ N.m.s}$ , pole pairs=2. A generator set is coupled to the motor as a load torque. Figure (8) shows the three-phase MLI output voltage for  $V/F=100/50$  with corresponding speed of 1400rpm.

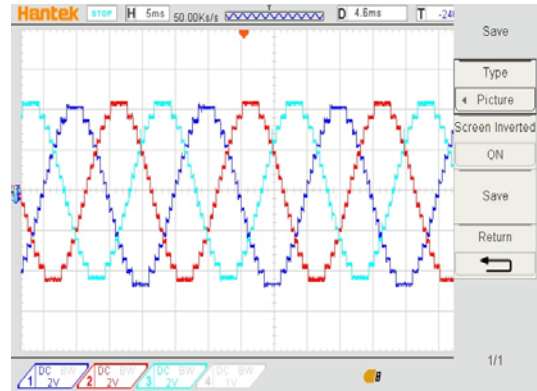


Fig.8. three-phase inverter output voltage for  $V/f=100/50$

The required  $120^\circ$  shift between the phases is shown in figure (9).

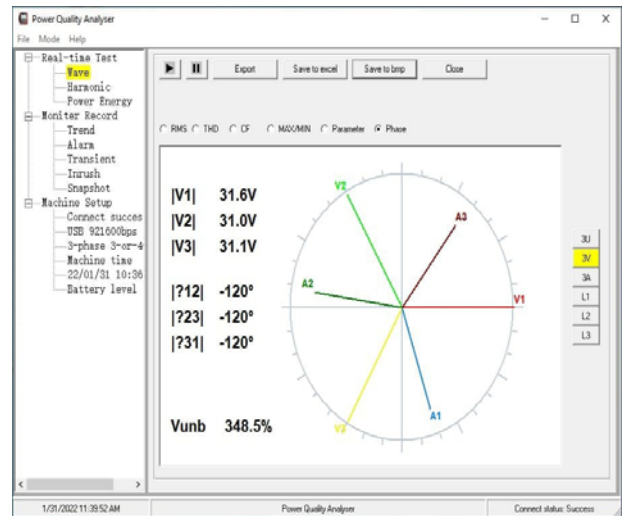


Fig.9.  $120^\circ$  shift between the phases

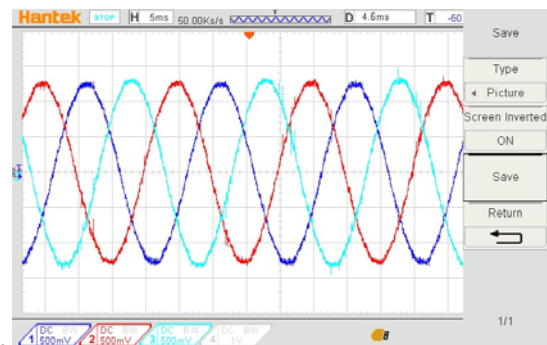


Fig.10. Three-phase inverter current for  $V/f=100/50$

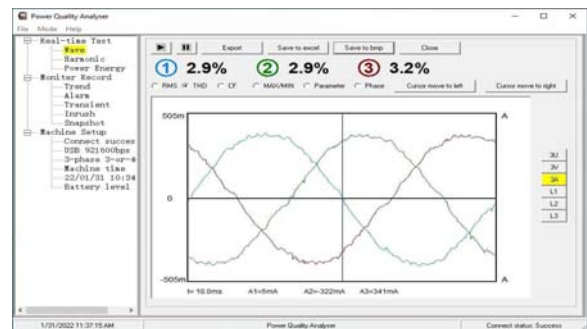


Fig.11. THD for three phase output voltage

The three-phase current from the MLI to the stator of the induction motor is shown in figure 10. The THD is shown to be around 3% as shown in figure 11.

The line-line voltage with 25 level steps is shown in figure (12) with its frequency spectrum. The first harmonic to show is 23<sup>rd</sup> as expected.

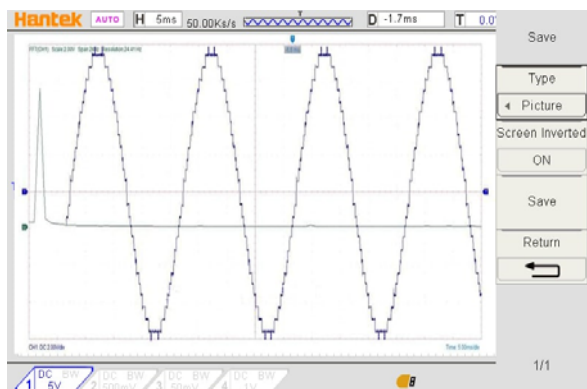


Fig.12. Line voltage of the three-phase inverter for V/f= 100/50

The corresponding motor speed in this case is 1450rpm and the load torque is 1Nm as shown in figure (13).



Fig.13. Load torque and corresponding speed for V/f=100/50

The second case of the speed is taken for V/f=70/35. The MLI three-phase output voltages and currents are shown in figure (14) and figure (15) respectively.

The corresponding speed is 1050rpm and the torque meter shows the value of 1Nm which is the same reading as for V/f=100/50 in figure (13). The third case for V/f=50/25, the MLI three-phase output voltages and currents are shown in figure (16) and figure (17) respectively.

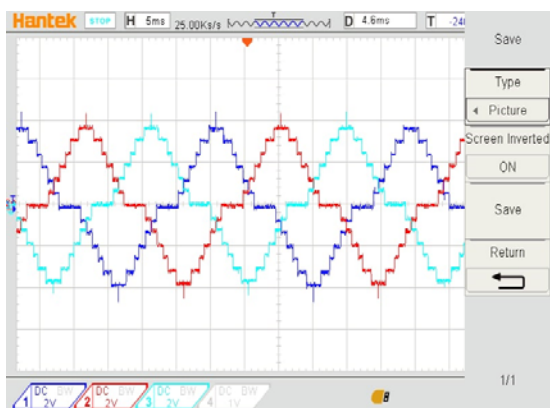


Fig.14. Three phase inverter output voltage for V/f=70/35

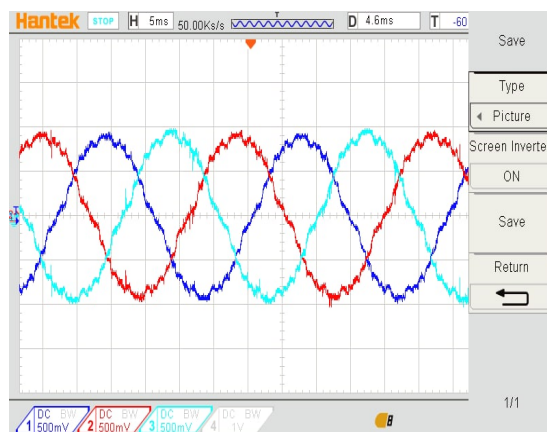


Fig.15. Three phase inverter current for V/f=70/35

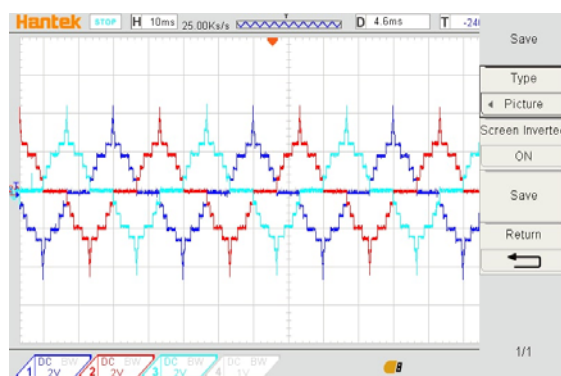


Fig.16. Three phase inverter output voltage for V/f=50/25

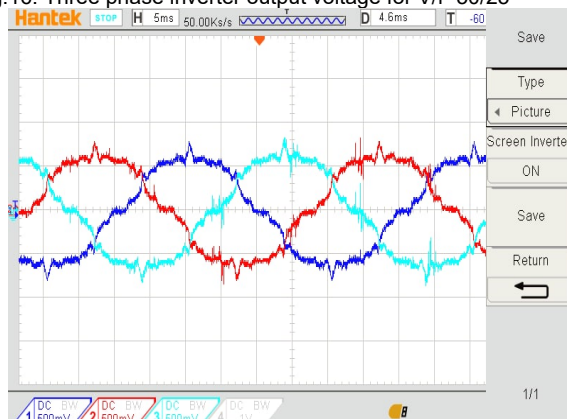


Fig.17. Three phase inverter current for V/f=50/25

The corresponding speed is 600rpm and the torque meter shows the value of 1Nm which is the same reading as for previous two cases as shown in figure (13). The results for the three v/f cases verifies that the motor torque is kept constant and at its maximum value as long the motor is operated in the linear region of v/f ratio as stated and previously shown in figure (1).

## 7. Conclusions

A three-phase induction motor driven by three phase inverter using the V/F strategy is talked in this work. The GWO algorithm is employed to optimize the triggering instants for the MOSFET switches to minimize the THD in the output voltage. A practical system is built, and the control signals are derived from 3E spartan FPGA kit using VHDL programming language. The results show that the torque is kept constant and at its maximum value for different values of V/F. The optimized triggering angles drives the THD of the output voltage to very small values.

Authors : Assistant prof. Taha Ahmed Hussein, Northern Technical University, Iraq, Email : taha.hussien@ntu.edu.iq  
 Assistant prof. Dr. Laith A. Mohammed , Northern Technical University, Iraq, Email : laith.akram@ntu.edu.iq  
 M.Sc. student Laith A. Hamdy , Northern Technical University  
 Email: laith.hamdy@ntu.edu.iq

## REFERENCES

- [1] H. P. Vemuganti, D. Sreenivasarao, S. K. Ganjikunta, H. M. Suryawanshi, and H. Abu-Rub, "A survey on reduced switch count multilevel inverters," *IEEE Open J. Ind. Electron. Soc.*, vol. 2, no. January, pp. 80–111, 2021, doi: 10.1109/OJIES.2021.3050214.
- [2] M. A. Hosseinzadeh, M. Sarebanzadeh, M. Rivera, E. Babaei, and P. Wheeler, "A Reduced Single-Phase Switched-Diode Cascaded Multilevel Inverter," *IEEE J. Emerg. Sel. Top. Power Electron.*, vol. 9, no. 3, pp. 3556–3569, 2021, doi: 10.1109/JESTPE.2020.3010793.
- [3] R. Palanisamy *et al.*, "A new multilevel DC-AC converter topology with reduced switch using multicarrier sinusoidal pulse width modulation," *Int. J. Power Electron. Drive Syst.*, vol. 11, no. 2, pp. 752–761, 2020, doi: 10.11591/ijpeds.v11.i2.pp752-761.
- [4] A. Taheri and H. Samsami, "New topology of a switched-capacitor-based multilevel inverter with a single DC power supply," *IET Power Electron.*, vol. 12, no. 6, pp. 1571–1584, 2019, doi: 10.1049/iet-pel.2018.5087.
- [5] R. Barzegarkhoo, E. Zamiri, M. Moradzadeh, and H. Shadabi, "Symmetric hybridised design for a novel step-up 19-level inverter," *IET Power Electron.*, vol. 10, no. 11, pp. 1377–1391, 2017, doi: 10.1049/iet-pel.2016.0558.
- [6] R. Bharti, M. Kumar, and B. M. Prasad, "V/F Control of Three Phase Induction Motor," *Proc. - Int. Conf. Vis. Towar. Emerg. Trends Commun. Networking, ViTECoN 2019*, no. May 2021, pp. 1–4, 2019, doi: 10.1109/ViTECoN.2019.8899420.
- [7] Ms. Priya Subhash Raichurkar, Prof. A Shravan Kumar, Prof. Seema G. Shirsikar, and Mr. Asif Liyakat Jamadar, "V/F Speed Control of 3 phase Induction Motor using Space Vector Modulation," *Int. J. Eng. Res.*, vol. V5, no. 01, pp. 735–742, 2016, doi: 10.17577/ijertv5is010652.
- [8] A. Ghosh, A. K. Ray, M. Nurujjaman, and M. Jamshidi, "Voltage and frequency control in conventional and PV integrated power systems by a particle swarm optimized Ziegler–Nichols based PID controller," *SN Appl. Sci.*, vol. 3, no. 3, pp. 1–13, 2021, doi: 10.1007/s42452-021-04327-8.
- [9] P. P. Biswas, N. H. Awad, P. N. Suganthan, M. Z. Ali, and G. A. J. Amaratunga, "Minimizing THD of multilevel inverters with optimal values of DC voltages and switching angles using LSHADE-EpSin algorithm," *2017 IEEE Congr. Evol. Comput. CEC 2017 - Proc.*, pp. 77–82, 2017, doi: 10.1109/CEC.2017.7969298.
- [10] Taha A. Hussein "Multilevel level single phase inverter implementation for reduced harmonic contents , International Journal of Power Electronics and Drive System (JPEDS) Vol. 12, No. 1, Mar 2021, pp. 314~324 ISSN: 2088-8694, DOI: 10.11591/ijpeds.v12.i1.pp314-324
- [11] Laith A. Mohammed, Taha A. Husain, Ahmed M. T. Ibraheem "Implementation of SHE-PWM technique for single-phase inverter based on Arduino "International Journal of Electrical and Computer Engineering (IJECE) Vol. 11, No. 4, August 2021, pp. 2907–2915 ISSN: 2088-8708, DOI: 10.11591/ijece.v11i4.pp2907-2915
- [12] Laith A. Mohammed Alsaqal, Ahmed M. T. Ibraheem Alnaib, and Omar Talal Mahmood, "Compression of Multiple Modulation Techniques for Various Topologies of Multilevel Converters For Single Phase AC Motor Drive", *International Journal of Power Electronics and Drive Systems (JPEDS)*, Vol. 10, No. 2, June 2019.
- [13] M. N. Hamidi, D. Ishak, M. A. A. M. Zainuri, and C. A. Ooi, "Multilevel inverter with improved basic unit structure for symmetric and asymmetric source configuration," *IET Power Electron.*, vol. 13, no. 7, pp. 1445–1455, 2020, doi: 10.1049/iet-pel.2019.0916.
- [14] C. Dhanamjayulu, D. Prasad, S. Padmanaban, P. K. Maroti, J. B. Holm-Nielsen, and F. Blaabjerg, "Design and Implementation of Seventeen Level Inverter with Reduced Components," *IEEE Access*, vol. 9, pp. 16746–16760, 2021, doi: 10.1109/ACCESS.2021.3054001.
- [15] J. Venkataramanaiah, Y. Suresh, and A. K. Panda, "A review on symmetric, asymmetric, hybrid and single DC sources based multilevel inverter topologies," *Renew. Sustain. Energy Rev.*, vol. 76, no. March, pp. 788–812, 2017, doi: 10.1016/j.rser.2017.03.066.
- [16] M. D. Siddique, S. Mekhilef, N. M. Shah, and M. A. Memon, "Optimal Design of a New Cascaded Multilevel Inverter Topology With Reduced Switch Count," *IEEE Access*, vol. 7, pp.24498–24510,2019,doi:10.1109/ACCESS.2019.2890872.
- [17] Rakan Khalil Antar, Taha Ahmed Hussein, Abdallah Mohamed Abdullah " Design and implementation of reduced number of switches for new multilevel inverter topology without zero-level state" , International Journal of Power Electronics and Drive Systems (JPEDS) Vol. 13, No. 1, March 2022, pp. 401~410 ISSN: 2088-8694, DOI: 10.11591/ijpeds.v13.i1.pp401-410
- [18] P. Niu, S. Niu, N. liu, and L. Chang, "The defect of the Grey Wolf optimization algorithm and its verification method," *Knowledge-Based Syst.*, vol. 171, pp. 37–43, 2019, doi: 10.1016/j.knsys.2019.01.018.
- [19] M. Norambuena, J. Rodriguez, S. Kouro, and A. Rathore, "A novel multilevel converter with Reduced switch count for low and medium voltage applications," *2017 IEEE Energy Convers. Congr. Expo. ECCE 2017*, vol. 2017-Janua, pp. 5267–5272, 2017, doi: 10.1109/ECCE.2017.8096884.
- [20] X. Yuan, "Derivation of Voltage Source Multilevel Converter Topologies," *IEEE Trans. Ind. Electron.*, vol. 64, no. 2, pp. 966–976, 2017, doi: 10.1109/TIE.2016.2615264
- [21] Z. B. Duranay, H. Guldemir, and S. Tuncer, "Implementation of a novel multilevel converter with Reduced switch count for low and medium voltage applications," *2017 IEEE Energy Convers. Congr. Expo. ECCE 2017*, vol. 2017-Janua, pp. 5267–5272, 2017, doi: 10.1109/ECCE.2017.8096884.
- [22] L. A. Mohammed, "Voltage to Frequency Speed Control of Induction Motor using Cascaded Multilevel inverter," *2nd Int. Conf. Electr. Commun. Comput. Power Control Eng. ICECCPCE 2019*, pp. 148–152, 2019, doi: 10.1109/ICECCPCE46549.2019.203764.
- [23] Taha A. Hussein, Laith A. Mohammed " Detailed Simulink implementation for induction motor control based on space vector pulse width modulation SVPWM" , Indonesian Journal of Electrical Engineering and Computer Science Vol. 22, No. 3, June 2021, pp. 1251~1262 ISSN: 2502-4752, DOI: 10.11591/ijeecs.v22.i3.pp1251-1262
- [24] S. Kakar, S. B. M. Ayob, A. Iqbal, N. M. Nordin, M. Saad Bin Arif, and S. Gore, "New Asymmetrical Modular Multilevel Inverter Topology with Reduced Number of Switches," *IEEE Access*, vol. 9, no. Mli, pp. 27627–27637, 2021, doi: 10.1109/ACCESS.2021.3057554.
- [25] H. Akagi, "Multilevel Converters: Fundamental Circuits and Systems," *Proc. IEEE*, vol. 105, no. 11, pp. 2048–2065, 2017, doi: 10.1109/JPROC.2017.2682105.
- [26] Laith A. Mohammed " Voltage to Frequency Speed Control of Induction Motor using Cascaded Multilevel inverter" , 2nd international conference on electrical, communication, computer, power and control engineering iceccpce19, 13-14 february, 2019 | mosul, iraq
- [27] Ms. Priya Subhash Raichurkar, Prof. A Shravan Kumar, Prof. Seema G. Shirsikar, and Mr. Asif Liyakat Jamadar, "V/F Speed Control of 3 phase Induction Motor using Space Vector Modulation," *Int. J. Eng. Res.*, vol. V5, no. 01, pp. 735–742, May 2015 , doi: 10.17577/ijertv5is010652.
- [28] R. Bharti, M. Kumar, and B. M. Prasad, "V/F Control of Three Phase Induction Motor," *Proc. - Int. Conf. Vis. Towar. Emerg. Trends Commun. Networking, ViTECoN*, pp. 1–4, 2019, doi: 10.1109/ViTECoN. March 2019.8899420.
- [29] J. S. Wang and S. X. Li, "An Improved Grey Wolf Optimizer Based on Differential Evolution and Elimination Mechanism," *Sci. Rep.*, vol. 9no. 1, pp. 1–21, 2019, doi:10.1038/s41598-019-43546-3
- [30] H. D. Laslo and T. Varodi, "the Reduction of Total Harmonic Distortion for the Multilevel Converter Using Genetic Algorithms Optimization Method," vol. 12, no. 1, pp. 7–21, 2018.
- [31] J. A. Gallardo, J. L. Diaz, and A. Pardo, "Particle Swarm Optimization to minimize THD in Multilevel Inverters," vol. 2, no. c, pp. 22–29, 2017.